Enhancing the Electronic Structure of Ni-based Electrocatalysts through N Element substituting for the Hydrogen Evolution Reaction

Yibin Yang, [a] Xin Jin [b], Fangyang Zhan *[c] and Yang Yang *[d]

a. Chemical Pollution Control Chongqing Applied Technology Extension Center of Higher Vocational Colleges, Chongqing Industry Polytechnic College, Chongqing 401120, PR China

b. College of Physics and Electronic Engineering, Chongqing Normal University, Chongqing 401331, P. R. China

c. Institute for Structure and Function & Department of Physics, Chongqing University, Chongqing 400044, P. R. China。

d. Key Laboratory of Chemical Additives for China National Light Industry, College of Chemistry and Chemical Engineering, Shaanxi University of Science & Technology, 710021 Xi'an, China.

AUTHOR INFORMATION

Corresponding Author

Name: Fangyang Zhan; Yang Yang

E-mail: zhan_fyang@cqu.edu.cn; yyang399@sust.edu.cn

Notes

The authors declare no competing financial interest.

Experimental

Chemical and Materials: $NiCl_2 \cdot 6H_2O$, urea and HCl were purchased from Aladdin Chemical Reagent Co., Ltd., Nickel foam were purchased from CeTech Co., Ltd. All products which were purchased were directly used without further purification.

Treatment of nickel foams: The nickel foams (NF), meticulously trimmed to the appropriate dimensions, was thoroughly cleansed with absolute alcohol for a duration of 10 minutes. This step was crucial to eliminate any organic compounds present on the surface. Subsequently, the NF was dried at a temperature of 60 ℃ for 2 h. Once dried, the NF was immersed in concentrated hydrochloric acid within an ultrasonic bath for a brief 5 minutes, a process designed to eradicate the layer of surface oxides. Following this, the NF was subjected to a series of 3 min each time washes using deionized water. As a final step, the nickel foam was submerged in deionized water for preservation purposes. This comprehensive process ensures the NFs is thoroughly prepared and preserved for future use.

Synthesis of $Ni(OH)_2$ grown on nickel foams ($Ni(OH)_2$/NF): In the conventional method, $NiCl_2 \cdot 6H_2O$ (1.45 g) and Urea (1.40 g) were dissolved in 35 mL of distilled water, resulting in a transparent solution after stirring. This aqueous solution, along with the NF, was then transferred into a 50 mL Teflon-lined stainless-steel autoclave. The autoclave was sealed and sustained at 120° C for 8 h, followed by a rapid cooling to room temperature within 15 min using a cooling water system. The $Ni(OH)_2$ formed on the NF was thoroughly rinsed multiple times with distilled water, aided by

ultrasonication. Subsequently, it was dried at 80°C for 6 h to yield the 3D $Ni(OH)_2$/NF composite.

Synthesis of NiO grown on nickel foams (NiO/NF): Initially, a synthesized 3D $Ni(OH)_2$/NF specimen was positioned within a tube furnace. Subsequently, the temperature of furnace was escalated to 400 °C at 10 °C/min in an air-flowing environment. This temperature was sustained for a duration of 2 h, after which the system was permitted to revert to ambient temperature, resulting in the formation of the 3D NiO/NF composite.

Synthesis of Ni_3N grown on nickel foams (Ni3N/NF): Initially, a synthesized 3D $Ni(OH)_2$/NF sample was positioned within a tube furnace. Subsequently, the furnace was escalated to 400 °C at 10 °C/min, under a continuous flow of NH_3 atmosphere. This temperature was sustained for a duration of 3 h. Following this, the furnace was permitted to cool down to ambient temperature, resulting in the formation of the 3D Ni_3N/NF composite.

Materials Characterizations: The collection of X-ray diffraction (XRD) data was executed utilizing Cu-kα radiation (λ=1.5418 Å) via a Shimadzu ZD-3AX diffractometer. A Fourier transform infrared (FT-IR) spectrophotometer (Bruker Tensor 27) was employed for spectroscopic analysis within the range of 400 to 4000 cm-1. Transmission electron microscopy (TEM) and Energy dispersive X-ray spectroscopy (EDS) assessments were conducted using a FEI Tecnai G2 F20 electron microscope, operating at an accelerating voltage of 200 kV. The Nova 400 Nano-SEM scanning electron microscope was utilized for Scanning electron microscopy (SEM)

measurements. X-ray photoelectron spectroscopy (XPS) analysis was performed using a Thermal ESCALAB 250 spectrometer equipped with an Mg kα X-ray source. Inductively coupled plasma optical emission spectrometry (ICP-OES) was carried out on acid-digested LDH samples using an iCAP 6300 Duo.

Electrochemical characterizations: The electrochemical evaluations were executed utilizing a CHI 660E electrochemical workstation (CH Instruments, Inc., Shanghai) with a tri-electrode configuration. The fabricated samples functioned as the active electrode, while a platinum electrode and a saturated Ag/AgCl electrode were employed as auxiliary and reference electrodes, respectively. Throughout the assessments, potential calibrations were made to the reversible hydrogen electrode (RHE) by modulating the pH value: E(RHE) = E(Ag/AgCl) + 0.197 V + 0.059 × pH. To generate all polarization curves, linear sweep voltammetry (LSV) was conducted within a range of -0.9 to -1.5 V versus Ag/AgCl at a scanning velocity of 5 mV s^{-1}. All polarization curves were rectified for the iR drop at 85%. The computation of current density was contingent on the geometric expanse of the electrode. Electrochemical impedance spectroscopy (EIS) was performed at -1.2 V versus Ag/AgCl, spanning a frequency spectrum from 0.1 Hz to 100 kHz.

Computational method：The spin polarized periodic density functional theory calculations were performed using the Vienna Ab-initio Simulation Package (VASP) code. For improving the calculation efficiency, core electrons were replaced by the projector augmented wave (PAW) pseudo-potentials. The generalized gradient approximation of the Perdew-Burke-Ernzernhof (PBE) functional was utilized for the

exchange and correlation. The Brillouin zone integrations were carried out with a 3 × 3 × 3 Monkhorst-Pack grid. The U value is 4.3 eV for Ni with the literatures. [1-3] The kinetic energy cutoff of 450 eV was used. A force tolerance, energy tolerance per atom and maximum displacement was set to 0.01 eV $Å^{-1}$, 5.0 × 10 eV^{-7} and 5.0 × 10^{-4} Å, respectively.

DFT：Reaction free energy of HER

The four-electron OER process in the alkaline medium,

$$2H^{+}+2e^{-}\rightarrow H_2(g),$$

which is divided into four elementary steps, which involve the binding of three oxygen-containing intermediates on the surface of catalyst:

$$* + H^{+}+ e^{-}\rightarrow *H$$

$$* H+ H^{+} + e^{-}\rightarrow *+ H_2(g)$$

where * denotes the active site on the catalyst surface. The adsorption free energy of intermediate and reaction free energy of elementary step were calculated according to the computational hydrogen electrode (CHE) model developed by J. K. Nørskov *et al*.,[4-6] where the reversible hydrogen electrode (RHE) is used as reference electrode. In this model, the Gibbs free energy is calculated by

$$\Delta G = \Delta E_{\mathrm{DFT}} + T\Delta S + \Delta \mathrm{ZPE} + \Delta G_U + \Delta G_{\mathrm{pH}}$$

where ΔE_{DFT} is the change of total energy calculated by DFT, ΔS is change of entropy term, T is operating temperature and is set as room temperature (298.15 K), and ΔZPE is the variation on the zero-point energy, which is calculated by frequency calculations in VASP; $\Delta G_U = neU$ is the correction of the applied electrode potential (U) when n

electrons are transferred, and $\Delta G_{pH} = pH \times k_B T \ln 10$ (k_B, the Boltzmann constant) is the pH correction of the aqueous solution, and these two correction terms are neglected as they have same effect on the equilibrium potential and the onset potential of HER, but the effect is canceled out when overpotential (η) is determined vs. RHE. Within the CHE model, the free energy of proton-electron pair is equal to that of half a hydrogen gas of 1 bar ($H^+ + e^- = 1/2H_2(g)$ is in equilibrium), then we have

$$G(OH^-) - G(e^-) = 1/2G(H_2, g)$$

As for the adsorption free energy of *OH, *O and *OOH, they are taken as the free energy of stoichiometrically appropriate amounts of $H_2O(g)$ and $H_2(g)$,[7] given that $G(H_2O, l) = G(H_2O, g, 298.15\ K, 0.035\ bar)$,[6] we have

$$\Delta G_{*OH} = G(*OH) - [G(H_2O, g) - 1/2G(H_2, g)]$$

$$\Delta G_{*O} = G(*O) - [G(H_2O, g) - G(H_2, g)]$$

$$\Delta G_{*OOH} = G(*OOH) - [2G(H_2O, g) - 3/2G(H_2, g)]$$

where G(*OH), G(*O) and G(*OOH) are the free energies of absorbed state of reaction intermediates, corrected with zero-point energy. The atoms of the surface are fixed during the zero-point energy calculations. The entropies of absorbate and the catalysts are neglected. We then get the reaction free energies of the four elementary steps of OER: $\Delta G_1 = \Delta G_{*OH}$, $\Delta G_2 = \Delta G_{*O} - \Delta G_{*OH}$, $\Delta G_3 = \Delta G_{*OOH} - \Delta G_{*O}$, $\Delta G_4 = 4.96\ eV - \Delta G_{*OOH}$, and the step that has the most positive free energy is the potential-determining step (PDS), which gives the theoretical overpotential of OER (η) derived as $\eta = \Delta G_{PDS}/e - 1.23\ V$.

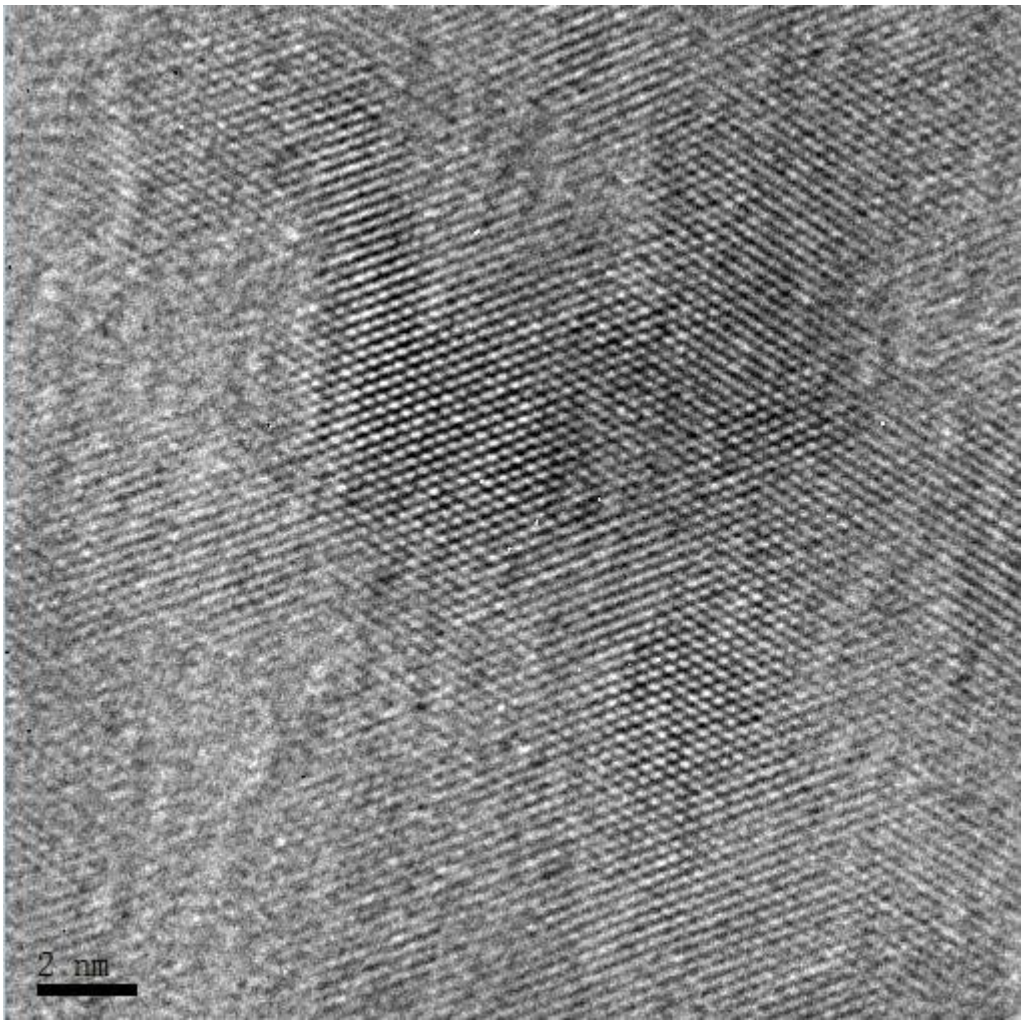

Figure S1 HRTEM of the Ni_3N nanosheets showing the lattice fringes.

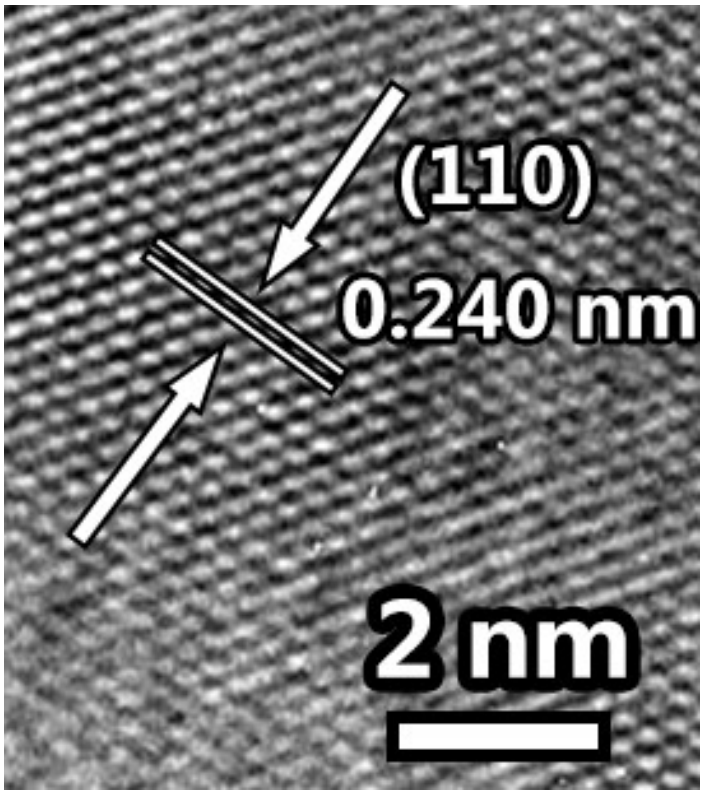

Figure S2 HRTEM of the Ni_3N nanosheets showing the lattice fringes.

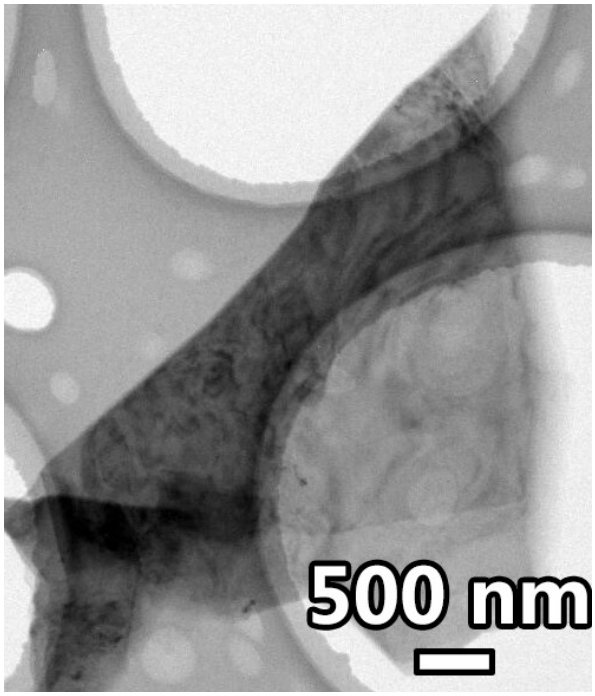

Figure S3 TEM image of Ni_3N.

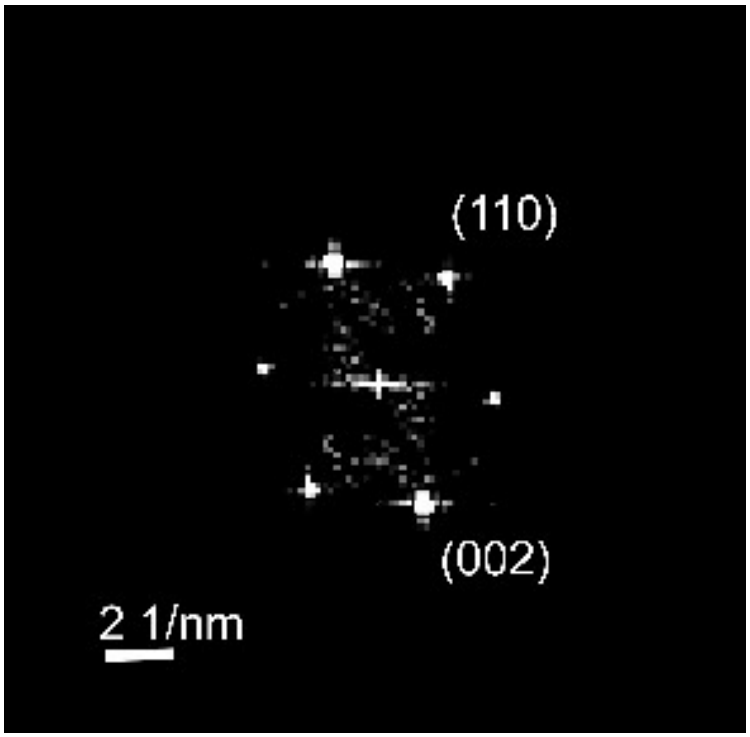

Figure S4 SAED pattern of the Ni_3N nanosheets.

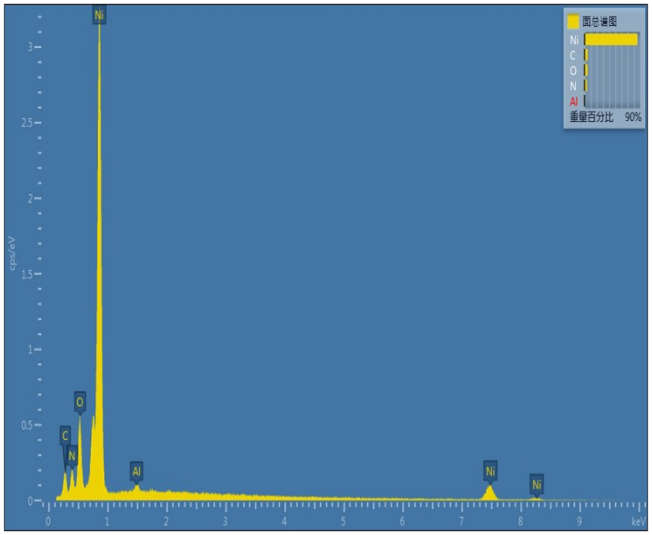

Figure S5 EDX patterns and the corresponding element molar ratio of Ni_3N.

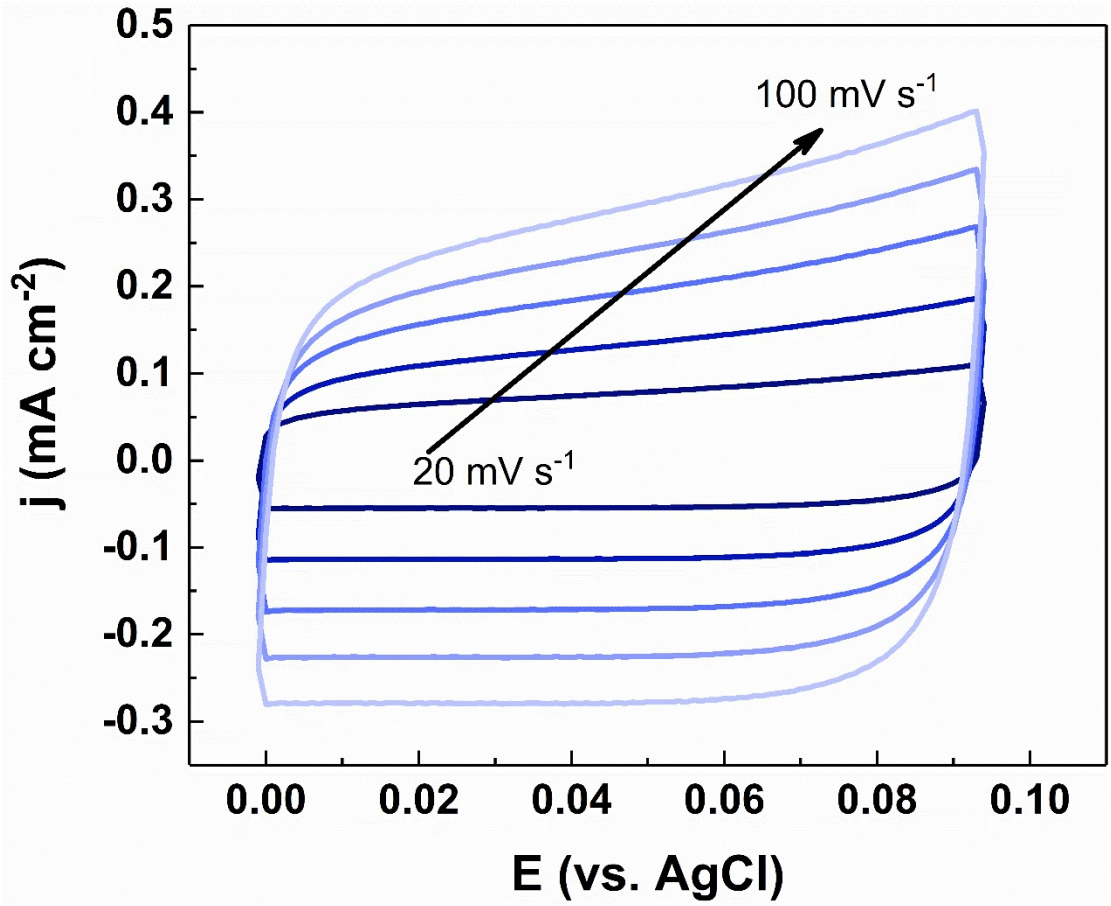

Figure S6 ECSA of $Ni(OH)_2$/NF

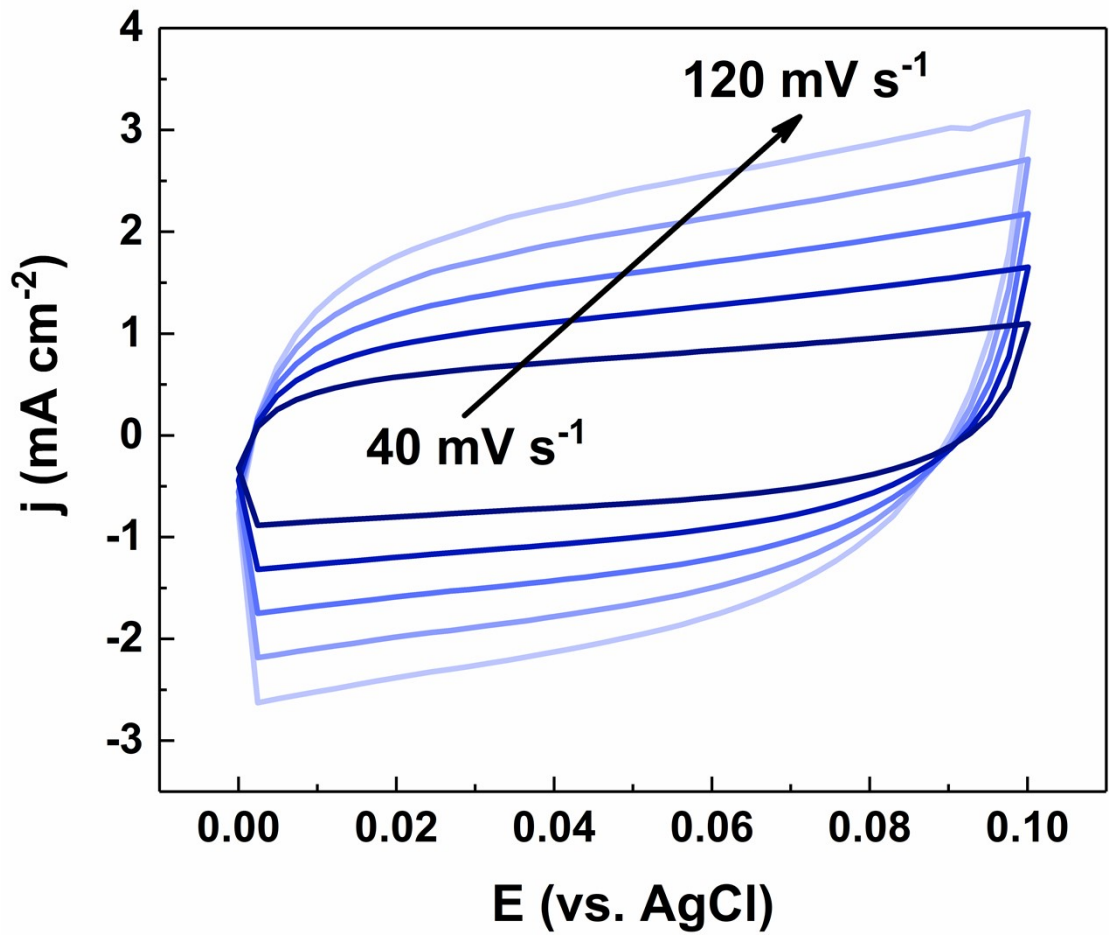

Figure S7 ECSA of Ni_3N/NF

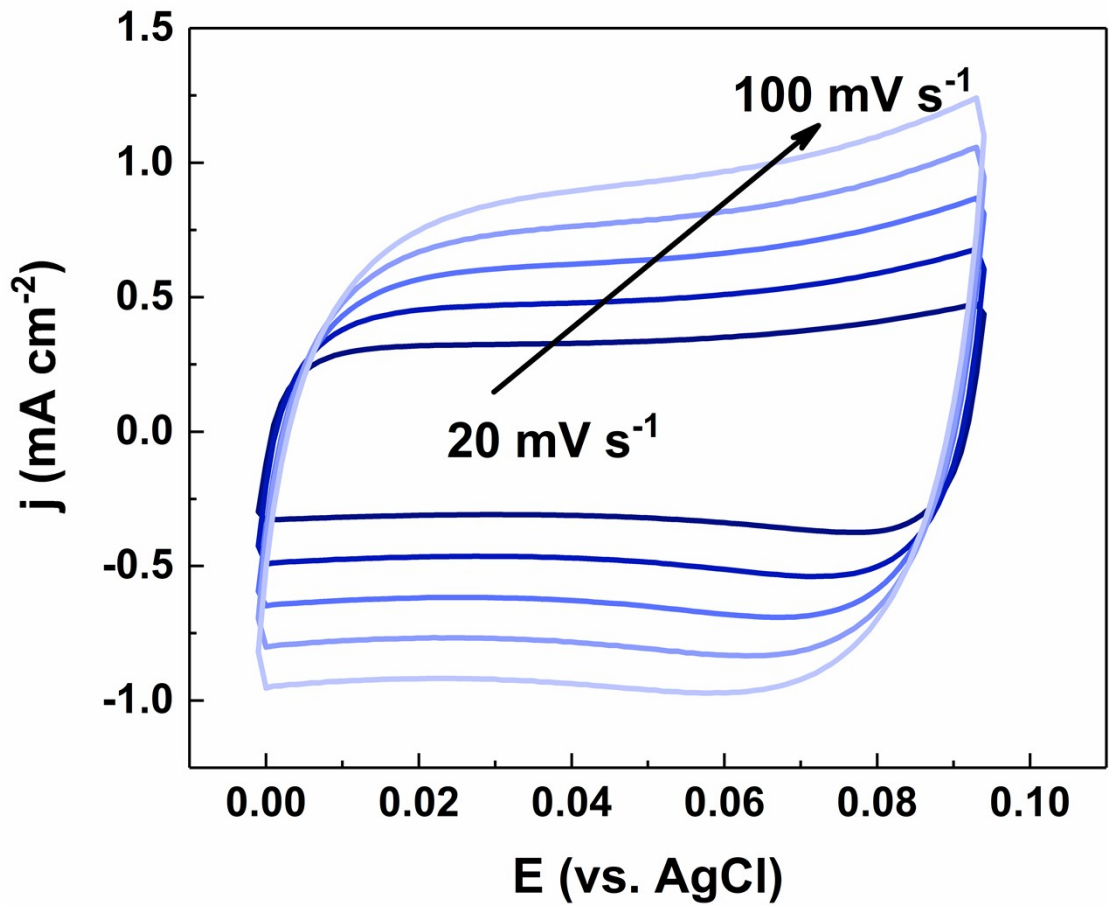

Figure S8 ECSA of NiO/NF.

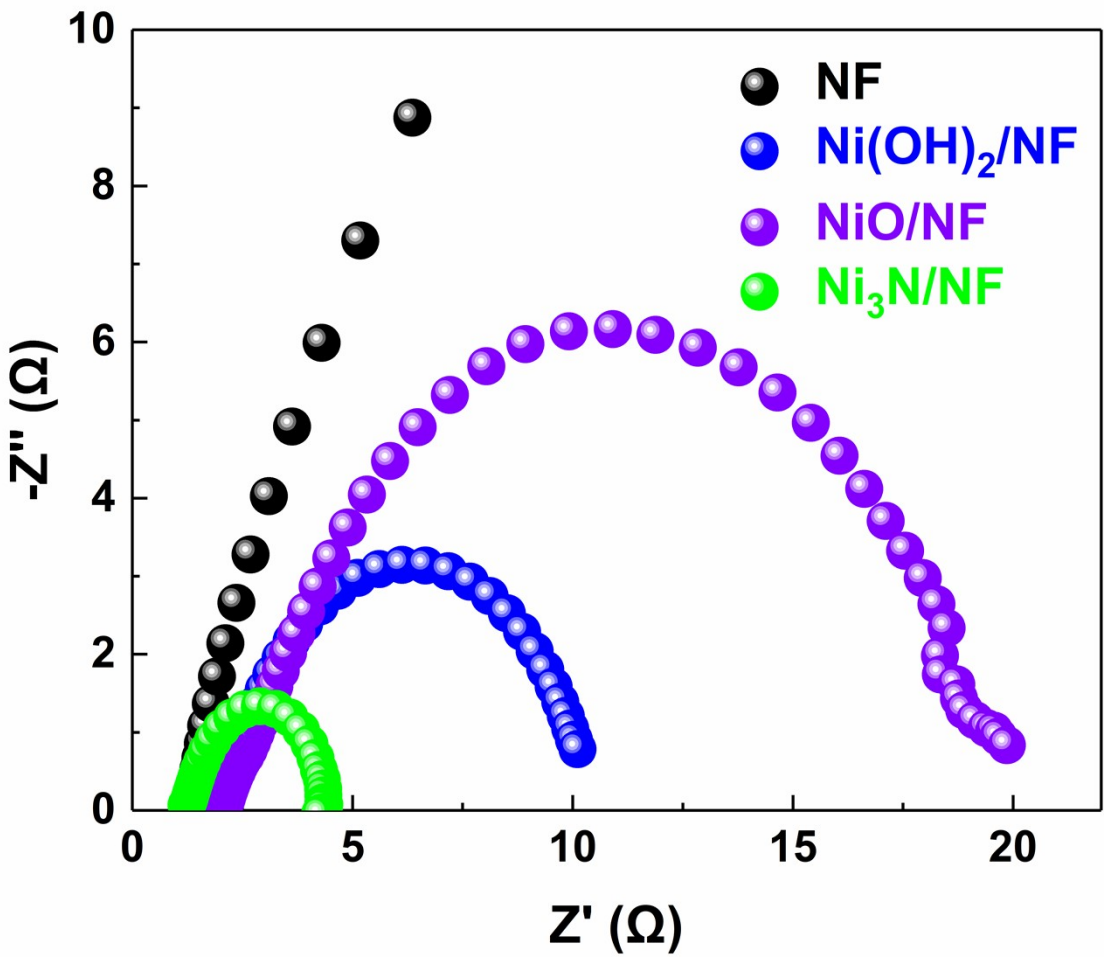

Figure S9 The EIS curves of Ni_3N/NF, NiO/NF and $Ni(OH)_2$/NF, respectively.

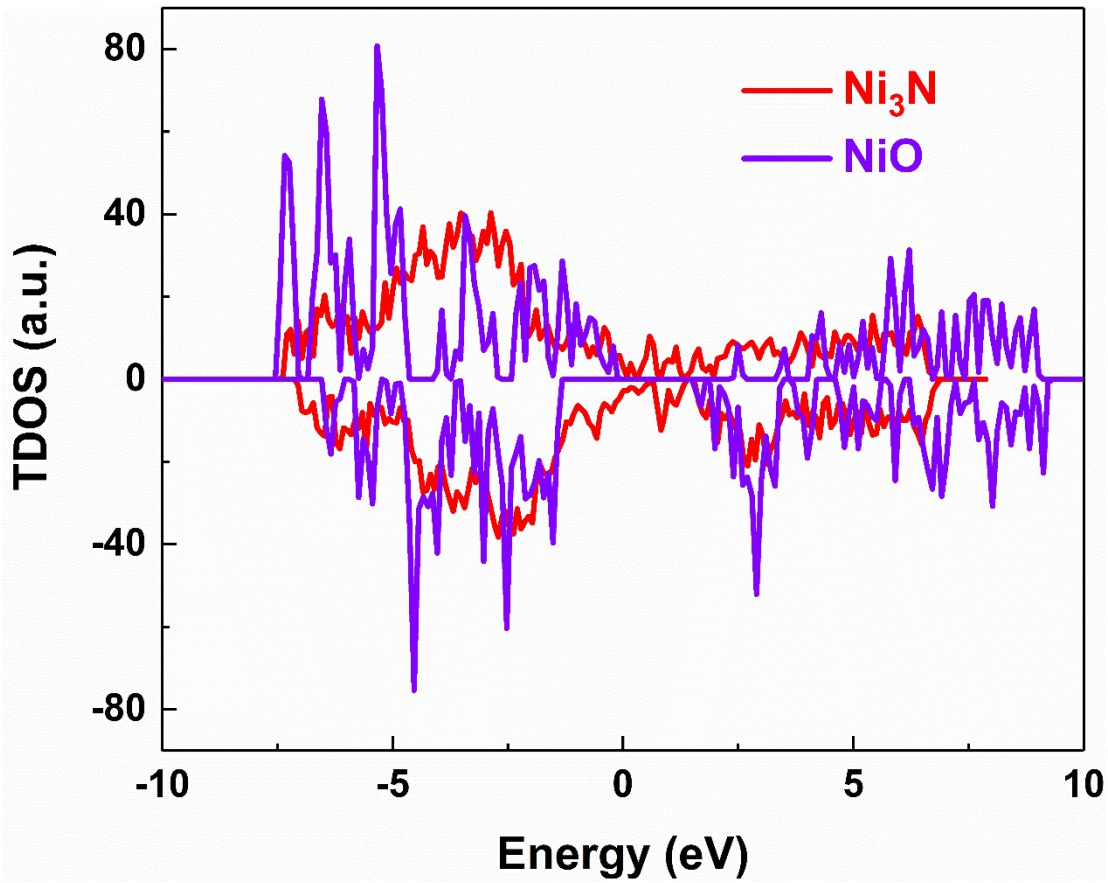

Figure S10 TDOS of Ni_3N and NiO, respectively.

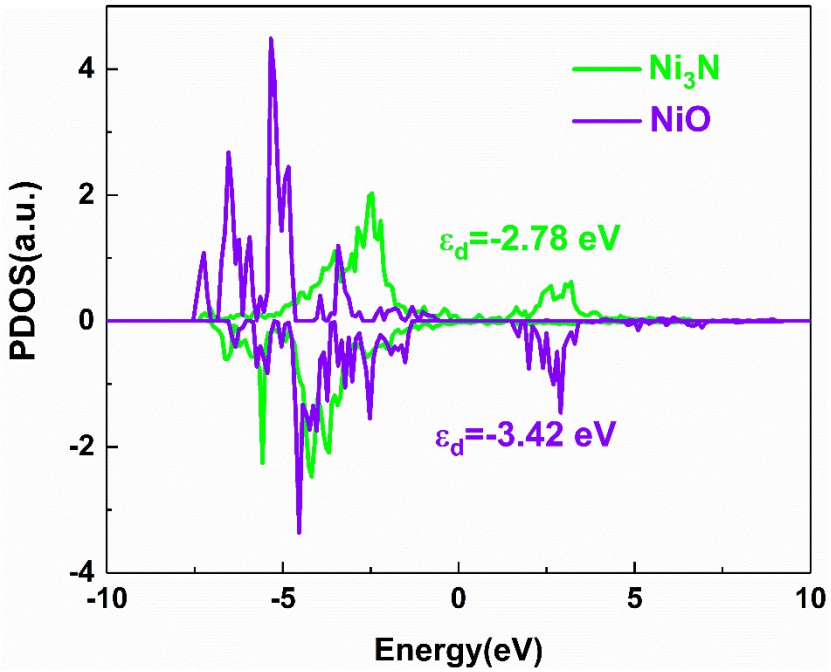

Figure S11 PDOS of Ni 3d in Ni_3N and NiO, respectively.